Physics IA

The Fluid Dynamics of a Spherical Object

How does Temperature of the fluid medium in laminar flow affect the drag force on a spherical body in linear motion?

***Word Count**: 2860*

Contents

Abstract

We will discuss the effects of change in the magnitude of **temperature** on the **Air Drag/Fluid Resistance** of a **spherical** body. We shall accomplish this by collecting raw data on the measurement of **drag force** with respect to **temperature** under certain controlled spaces with **defined standard initial conditions**.

1 Introduction

I have chosen this research question because the fundamental relation between the **mechanics of fluid flow**, its **complex dynamics** and its **excruciating difficulty in possibly modeling** this behavior has led me to explore this field.

2 Aim

To **collect experimental raw data** relating to the variation in **drag force** with the variation in **temperature** in a lab controlled setting of a **fluid medium** flow on a **spherical object** and to compare it with **computer simulations** of the same and hence study its **different states** and calculate the value the **inconsistencies** in **accuracy** of the **mathematically modeled computer simulation** to that of the **actual experiment** and vice-versa.

Research Question: *How does Temperature of the fluid medium in laminar flow affect the drag force on a spherical body in linear motion?*

3 Hypothesis

The **drag force** on the **spherical mass** would act **inversely proportional** to the the change in **temperature**, which means that with increase in temperature, the eminent drag force in impact on the spherical mass must decrease,**drag motion should be an inverse exponential compared to changes in temperature**.

4 Background Research

Before beginning this investigation we must first know some important facts, formulae, laws and be familiar with the concepts that are to be incorporated in this investigation.

4.1 Air Drag/Fluid Resistance

Air Drag/Fluid Resistance is the force acting opposite to the relative motion of any object moving in any fluid medium. Drag force is proportional to the **square of velocity**, as we are dealing with relatively high-speeds, which can be inferred from the small Reynolds's number.

Drag forces decrease the fluid velocity relative to the solid mass in the fluid's path.

The general Drag equation is mathematically defined as,

$$F_D = \frac{1}{2}\rho v^2 C_D A$$

Where F_D is the **Air/Fluid resistance** between the mass and the fluid, ρ is the **density of the fluid**, v is the **speed of the object** relative to the fluid, C_D is **velocity decay constant** (damping constant) and A is the **cross sectional area**.

Note: The**velocity decay constant**, C_D for the particular case that we are investigating, that is on **spherical bodies** has a set defined value of **0.47**.

4.2 Temperature dependence of thermal expansion coefficient

The thermal expansion coefficient is defined as,

$$\alpha_L = \frac{1}{L} \cdot \frac{\partial L}{\partial T}$$

Where, L is the **length measurement**, α_L is the **thermal expansion coefficient** in the dimension of the length measurement and T is the **temperature**.

Because, the length measurement that we are dealing with is Volume, the above equation reduces to,

$$\alpha_V = \frac{1}{V} \cdot \frac{dV}{dT}$$

This clearly indicates that α_V or the cubic expansion coefficient is a function dependent of temperature.

The below table encompasses the values of the cubic expansion coefficient of water at certain temperatures.

Temperature $°C$	Cubic thermal expansion coefficient $1/°C$
0	-0.000050
10	0.000088
20	0.000207
30	0.000303
40	0.000385
50	0.000457
60	0.000522
70	0.000582
80	0.000640
90	0.000695

4.3 Temperature dependence of density

We must know the fundamental relation between change in **temperature** on change in **density**.

We know that,

$$\rho = \frac{m}{V}$$

Where, ρ is the **density** of a particular substance, m is its **mass** and V is its **volume**.

Therefore, we have

$$\rho \propto \frac{1}{V}$$

Therefore, we infer that, **density** is **inversely proportional** to **volume** of the substance, here the **fluid**.

We have a equation for the temperature dependence on density [1]. That is,

$$\rho = \frac{\rho_0}{1 + \gamma \cdot \Delta T}$$

Where ρ is the **current density** of a particular substance, ρ_0 is the **initial density** of a particular substance, γ is the **volumetric/cubic thermal expansion coefficient** and ΔT is the change in the temperature from the initial state.

As $(1 + \gamma \cdot \Delta T)^{-1}$ is of the form $(1 + x)^{-1}$ we have,

$$(1 + \gamma \cdot \Delta T)^{-1} = 1 - (\gamma \cdot \Delta T) + (\gamma \cdot \Delta T)^2 - (\gamma \cdot \Delta T)^3 \cdots$$

If we ignore the higher order terms of $(\gamma \cdot \Delta T)$, as they are negligibly small, we have,

$$\rho = \rho_0 \left(1 - \gamma \cdot \Delta T\right)$$

Because γ is a function of T, $\gamma = \gamma_T$, therefore we have,

$$\rho = \rho_0 \left(1 - \gamma_T \cdot \Delta T\right)$$

4.4 Computer Simulation Software

To **model** the **drag force** on a **sphere in fluid flow**, we would need the aid of **computational technology**. Software's such MATLAB, Mathematica or some simple, eccentric computer programming language code in a emulatable script format, that would compute and yield solutions for necessary simulations that are required.

For the purpose of this investigation we shall be using a **MATLAB script**, to model and simulate the system.

5 Materials Required

- Huge Rectangular Glass Container
- Spherical Mass
- Thermometer (Digital)

- Fluid - **Water**

Note: In theory, the fluid utilized in this research could of arbitrary any substance with fluid properties. For the purpose of this investigation, we shall specifically use **water as the flow fluid**.

6 Variables

Physical Quantity	Symbol
Flow velocity	v
Drag coefficient	C_D
Temperature	T
Radius of spherical mass	r

Table 1: *General physical quantities employed in this investigation*

Note: In theory, the radius of the spherical mass and the flow velocity incorporated in research could of any arbitrary value. For the purpose of this investigation, we shall specifically use masses of radius 2.5×10^{-2} m and the flow velocity shall be set constant at 0.1 m/s.

Independent Variable	Dependent Variable	Controlled Variable
Temperature	Drag Force	Fluid medium
-	-	Radius of the spherical mass
-	-	Flow velocity

Table 2: Segregation of employed variables as IV, DV or CV

Note: The flow velocity, type of fluid medium and the radius of the mass is no longer variable as we have defined a set value to it.

7 Procedure

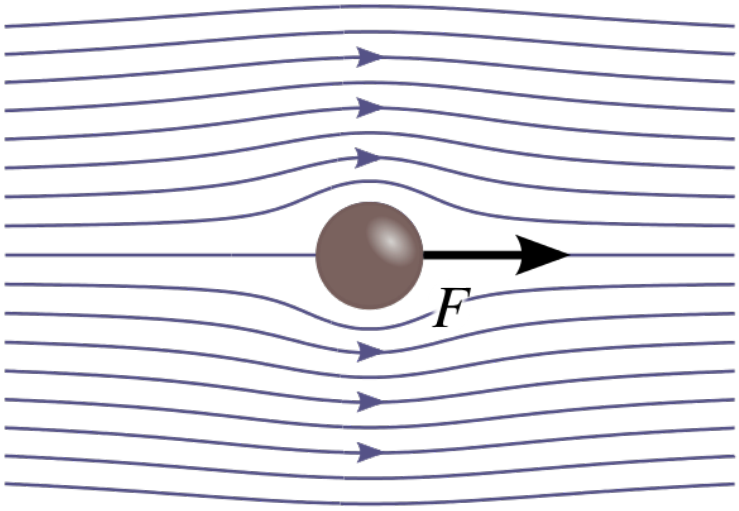

Figure 1: Diagram of the experiment carried down in this investigation

Using the materials specified in chapter 5, arrange the components as specified in figure 1 and make sure that the spherical mass is kept about at a fixed point.

Following which, pass through the fluid in a rectangular chamber while varying temperatures and obtain the drag force eminent on the spherical mass.

After the prior setup and during the experiment, the fluid must interact with the spherical mass in a manner depicted in figure 1.

8 Equations

8.1 Drag Equation for the Study

We know that,

$$F_D = \frac{1}{2}\rho v^2 C_D A$$

Also,

$$\rho = \rho_0 \left(1 - \gamma \cdot \Delta T\right)$$

Substituting the second equation in the first equation we have,

$$F_D = \frac{1}{2}\rho_0 v^2 C_D A \cdot (1 - \gamma \cdot \Delta T)$$

This equation can be rewritten as,

$$F_D = \frac{1}{2}\rho_0 v^2 C_D A \cdot (1 - \gamma \cdot (T - T_0))$$

When further reducing the variables to constants the following equation reduces to,

$$F_D = 4.61 \cdot 10^{-3} \cdot (1 - \gamma \cdot T)$$

Note: The initial density and temperature taken into account is 999.83 kg/m^3 and $0°C$ or 271.16 K.

Note: This equation is derived considering the Celsius unit for temperature difference as the least count for both the units (Celsius and Kelvin) are the same.

8.2 Equation used for further Investigation

The **equation used for further investigation** we shall be using in this investigation is:

$$F_D = 4.61 \cdot 10^{-3} \cdot (1 - \gamma_T \cdot T) \tag{1}$$

Where γ_T is the cubic thermal expansion coefficient of water and T is the magnitude of the temperature of water.

9 Data

9.1 Experimental Data

Observation number (x_i)	Temperature of Fluid (°C)	Drag Force (mN)
1	0	4.6100
2	10	4.6000
3	20	4.5906
4	30	4.6310
5	40	4.5270
6	50	4.5030
7	60	4.4606
8	70	4.4246
9	80	4.3666
10	90	4.3166

Table 3: Simulation data relating to changes in drag force relative to changes in the temperature of the fluid

Note: The above experimental data is the averaged mean of all data points from the data sets of the raw experimental data that can be found in the appendix A.

9.2 Simulation Data

Observation number (x_i)	Temperature of Fluid (°C)	Drag Force (mN)
1	0	4.61
2	10	4.60
3	20	4.59
4	30	4.56
5	40	4.53
6	50	4.50
7	60	4.46
8	70	4.42
9	80	4.37
10	90	4.32

Table 4: Simulation data relating to changes in drag force relative to changes in the temperature of the fluid

9.3 Processed Data

Temperature of Fluid (°C)	Avg. Exp. Drag Force (mN)	Sim. Drag Force (mN)
0	4.6100	4.61
10	4.6000	4.60
20	4.5906	4.59
30	4.6310	4.56
40	4.5270	4.53
50	4.5030	4.50
60	4.4606	4.46
70	4.4246	4.42
80	4.3666	4.37
90	4.3166	4.32

Table 5: Simplified version of processed data derived from tables 3 and 4

Note: The above data is the consolidated form of all data collected, by simulation and experiment throughout all data points from the data set.

10 Evaluation

Let $F_{D_{Exp}}$ be the experimental values and $F_{D_{Sim}}$ be the simulation values respectively for each and every case that we are investigating.

If we define F_{D_n} as the uncertainty in measurement in the experimental values of F_D, then F_{D_n} is mathematically defined as $\left|F_{D_{Sim}} - F_{D_{Exp}}\right|$

By using the above definitions we have,

10.1 Observation from Case 1 where $T = 10°\mathbf{C}$

By using equation 1, we see that the experimental and simulation value for F_{D_1} is 4.6 mN and 4.6 mN.

Therefore uncertainty in measurement for F_{D_1} in this case is ± 0 N.

10.2 Observation from Case 2 where $T = 20°\mathbf{C}$

By using equation 1, we see that the experimental and simulation value for F_{D_2} is 4.5906 mN and 4.59 mN.

Therefore uncertainty in measurement for F_{D_2} in this case is $\pm$*0.0006* mN.

10.3 Observation from Case 3 where $T = 30°\mathbf{C}$

By using equation 1, we see that the experimental and simulation value for F_{D_3} is 4.631 mN and 4.56 mN.

Therefore uncertainty in measurement for F_{D_3} in this case is $\pm$*0.071* mN.

10.4 Observation from Case 4 where $T = 40°\mathbf{C}$

By using equation 1, we see that the experimental and simulation value for F_{D_4} is 4.527 mN and 4.53 mN.

Therefore uncertainty in measurement for F_{D_4} in this case is $\pm$*0.297* mN.

10.5 Observation from Case 5 where $T = 50°\mathbf{C}$

By using equation 1, we see that the experimental and simulation value for F_{D_5} is 4.503 mN and 4.5 mN.

Therefore uncertainty in measurement for F_{D_5} in this case is $\pm$*0.03* mN.

10.6 Observation from Case 6 where $T = 60°\mathbf{C}$

By using equation 1, we see that the experimental and simulation value for F_{D_6} is 4.4606 mN and 4.46 mN.

Therefore uncertainty in measurement for F_{D_6} in this case is $\pm$*0.0006* mN.

10.7 Observation from Case 7 where $T = 70°\mathbf{C}$

By using equation 1, we see that the experimental and simulation value for F_{D_7} is 4.4246 mN and 4.42 mN.

Therefore uncertainty in measurement for F_{D_7} in this case is $\pm$*0.0046* mN.

10.8 Observation from Case 8 where $T = 80°\mathbf{C}$

By using equation 1, we see that the experimental and simulation value for F_{D_8} is 4.3666 mN and 4.37 mN.

Therefore uncertainty in measurement for F_{D_8} in this case is $\pm$*0.0534* mN.

10.9 Observation from Case 9 where $T = 90°\mathbf{C}$

By using equation 1, we see that the experimental and simulation value for F_{D_9} is 4.3166 mN and 4.32 mN.

Therefore uncertainty in measurement for F_{D_9} in this case is $\pm$*0.0034* mN.

We further define, the average uncertainty in measurement across all cases that have been investigated to be,

$$\overline{F_{D_n}} = \frac{\sum_{n=1}^{n} F_{D_n}}{n} = \frac{F_{D_1} + F_{D_2} + F_{D_3} + F_{D_4} + F_{D_5} + F_{D_6} + F_{D_7} + F_{D_8} + F_{D_9}}{9}$$

Therefore we have,

$\overline{F_{D_n}} = 0.05112mN = 5.112 \times 10^{-6}N$

Upon observation, we see that the value of $\overline{F_{D_n}}$ we have found is not equal to 1, but is relatively very close, so we can say that we have some errors in calculating the **drag force versus temperature**.

Percentage uncertainty in measurement of **drag force versus temperature** is $\left|1 - \overline{F_{D_n}}\right| \cdot 100\% = \mathbf{5.112\%} \approx \mathbf{5.12\%}$

11 Analysis

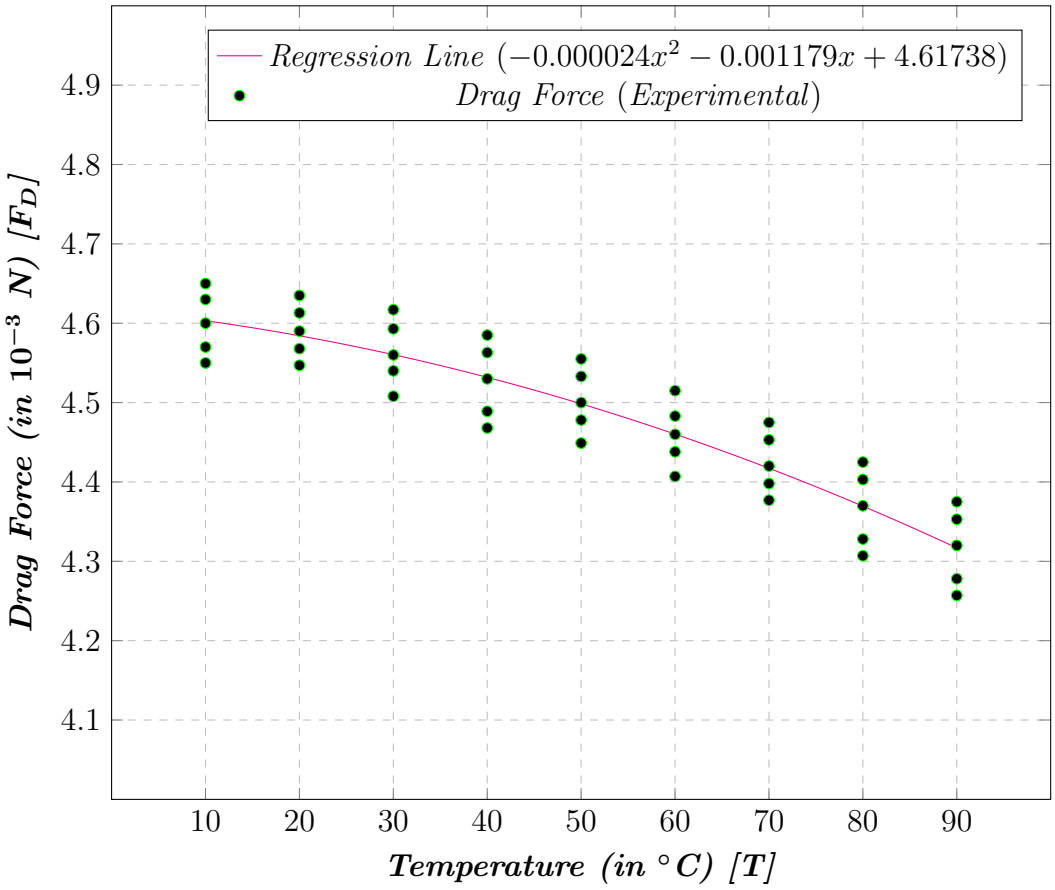

The above graph is the **scatter plot** of all **data points** within the **data set** of **experimentally collected values** with the **quadratic regression** of the same. A **quadratic regression** was utilized to plot the **line of best fit**, because a regression creates an **accurate model** of the system according to the data points and is a **mathematical function of each and every data point**. This was used rather than plotting an simple line between the **range** of the **maximum and minimum** values of the data points, as it would be similar to guesswork.

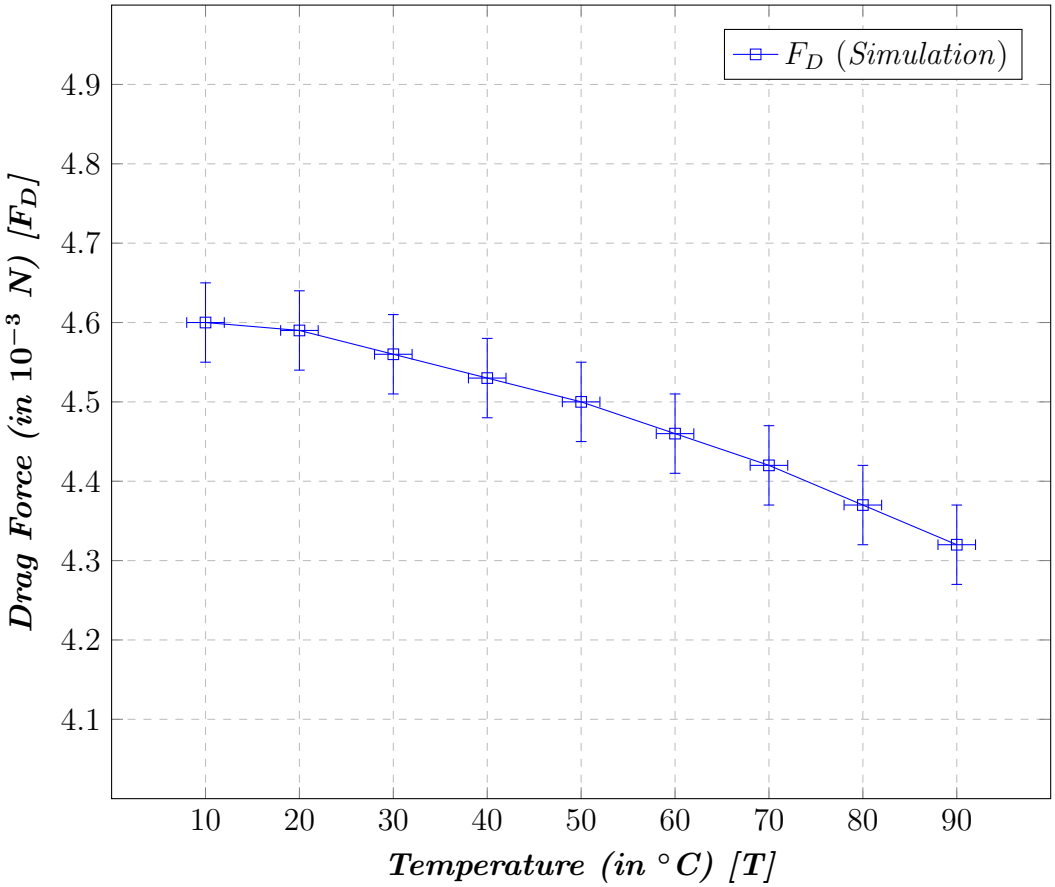

The above graph is the collection of single data points at specific intervals created with accordance to a simulation, based accurately on the **mathematical model** with **zero uncertainty**. On observation it looks evidently **similar to the quadratic regression line** from the previous graph, this is an **evidence that the experimental data collected was of least uncertainty and least errors** to an extent that was possible. The above graph also contains **ranges of values** in the form of **error bars** that show that the data points can range from a particular minimum to a particular maximum.

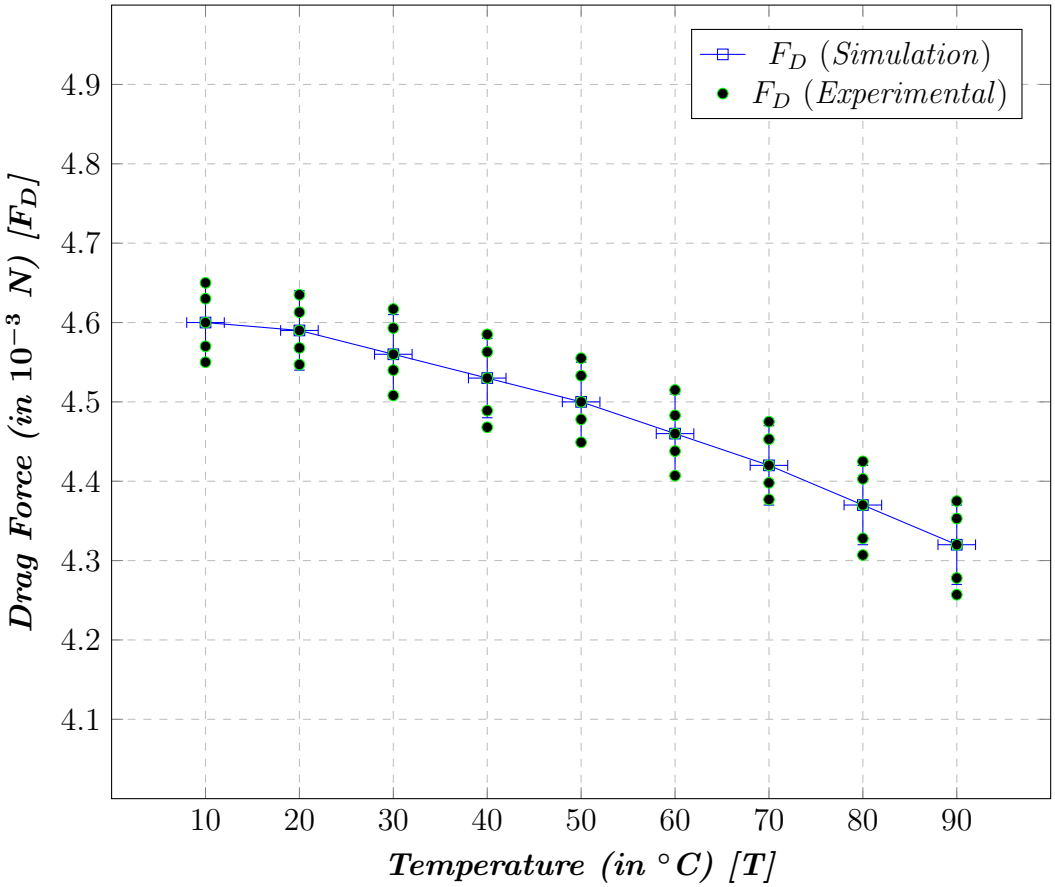

The above graph is a **culmination** of all the **experimentally collected data points** and the **data points collected via a simulation**. The **matching similarity** of the underlying graphs shows that the data is of much **reliability** and **devoid of errors**. According to the graph from the simulation, the error bars range lower than the maximum and minimum values (for most cases) of the experimentally collected values, indicating that such values are **outliers** and indicates that there has been **some errors and uncertainties** in the collection of data.

Upon close visual observation, we see that the difference in the plotted values of that of the **simulation** and **experimental values** of the **drag force** versus **temperature** from the **F-T** graph considering all data points are very **minute** to the extent that it would be right to say and consider that the experimental values are both **accurate** and **precise** in relation to that of the **literature/theoretical/simulation values**.

In order to model the system with accuracy, a **quadratic regression model** was utilized to model the **line of best-fit**.

It is evident from studying the system **numerically** and **graphically** that the system exhibits an **logarithmic decay** with time for the parameter that is being investigated. This points out to **one conclusion**, that the **parameter of the system undergoes logarithmic decay not linear decay**, according to their various **inert energies**.

Note: Due to constraints of resources, a **quadratic regression model** was utilized instead of a **logarithmic regression model**, but the part of the model that we are to analyze exhibits logarithmic decay over temperature and is **accurately similar** to a quadratic regression model when restricted in the domain from 10 ° C to 90 ° C.

This **contradicts** the **initial hypothesis** laid out prior to beginning the investigation as if, the system had to model **similarly** to the inverse exponential, then the logarithmic behavior that we observe would have not existed, but we see that this is not the case.

It would be right to say that the **initial hypothesis** that was laid out prior, beginning the experimentation was **incorrect** and is **not** a valid statement.

12 Limitations of Study

There are various limitations in this study/investigation as we have placed forth, certain strict conditions that make this system so constrained and disables us to expand our researching capability of this chaotic phenomenon. Conditions such as,

- Restricting the value of temperature domain from 10°Celsius to 90°Celsius
- Restricting the value of radius of the spherical body employed to 2.5×10^{-2} meters
- Restricting the the fluid type to only water

13 Safety Measures

The Safety Measures that were taken during the experimentation as as follows:

- Proper Laboratory equipment was utilized to conduct and collect data
- All Laboratory equipment was used in the presence of Lab instructors and Lab personnel

- The experiment was performed at a distance from the observer so as to, limit or eliminate the chances of any possible physical harm to the observer
- Any and all lab equipment was thoroughly examined for any defects that could potentially lead to safety hazards, before initiating experimentation
- It was made sure the experiment shall not be performed to highly flammable materials that would result in combustion from the frictional force onto the fluid medium

14 Sources of Error

There are various ways through which errors might have crept into our raw and ordered data, some of the possible sources of errors are:

1. Raw experimental data presented here in the investigation report is collected through lab experimentation, and there are chances that the data collected may have slight discrepancy in it
2. Insignificant random human errors by the observer, ie. parallax errors
3. Uncertainties that cannot be minimized due to lack of highly sophisticated equipment and materials used in the experiments in this investigation
4. Assumptions and certain conditions put forth on the the system to model its chaotic behavior

15 Conclusion

In this paper, I have shown the effects of changes in the **temperature** on an **spherical body** in a fluid medium in laminar flow on the **drag force** by collecting raw data relating to the above parameters, under certain controlled conditions as so to completely study the **motion/dynamics of the laminar fluid flow on a spherical body**.

I have also investigated the **validity** of our **initial hypothesis** and have come to a conclusion that our initial hypothesis was an **partially valid statement**.

I have also shown the possible **uncertainties in measurement** of **drag force** with respect to **temperature**.

Bibliography

[1] "Density of Liquids vs. Pressure and Temperature Change." *Engineering Tool Box*, Engineering Tool Box, www.engineeringtoolbox.com/fluid-density-temperature-pressure-d_309.html. Accessed 10 Oct. 2021.

[2] Cleynen, Olivier. "Streamlines Past a Sphere at Very Low Reynolds Numbers (Stokes or Creeping Flow)." *Wikimedia.Org*, Wikimedia, May 2014, commons.wikimedia.org/wiki/File:Flow_patterns_around_a_sphere_at_very_low_Reynolds_numbers.svg.

[3] "Volumetric (Cubic) Thermal Expansion." *Engineering Toolbox*, www.engineeringtoolbox.com/volumetric-temperature-expansion-d_315.html. Accessed 19 Dec. 2021.

[4] John Deyst, and Jonathan How. *16.61 Aerospace Dynamics*. Spring 2003. Massachusetts Institute of Technology: MIT OpenCourseWare, https://ocw.mit.edu. License: Creative Commons BY-NC-SA.

[5] "Classical Mechanics — Lecture 3." *YouTube*, uploaded by Stanford, 16 Dec. 2011, www.youtube.com/watch?v=3apIZCpmdls.

[6] Kreyszig, Erwin. *Advanced Engineering Mathematics*. Hoboken, NJ, United States, Wiley, 1972.

[7] Rowell, Derek. "State-Space Representation of LTI Systems." *2.14 Analysis and Design of Feedback Control Systems*, D. Rowell, 2002, pp. 1–18.

[8] J. Vandiver, and David Gossard. 2.003SC Engineering Dynamics. Fall 2011. Massachusetts Institute of Technology: MIT OpenCourseWare, https://ocw.mit.edu. License: Creative Commons BY-NC-SA.

Appendices

A Raw Experimental Data

Temperature of Fluid (°C) ±0.2	Trials (x_i)	Drag Force (mN) ±0.0005
10	1	4.595
	2	4.598
	3	4.6
	4	4.602
	5	4.605
20	1	4.5856
	2	4.5886
	3	4.5906
	4	4.5926
	5	4.5956
30	1	4.305
	2	4.308
	3	4.31
	4	4.312
	5	4.315

Table 6: *Raw Experimental data on the drag force from the temperature range of 10°C to 30°C*

Temperature of Fluid (°C) ±0.2	Trials (x_i)	Drag Force (mN) ±0.0005
40	1	4.522
	2	4.525
	3	4.527
	4	4.529
	5	4.532
50	1	4.498
	2	4.501
	3	4.503
	4	4.505
	5	4.508
60	1	4.455
	2	4.458
	3	4.46
	4	4.462
	5	4.465

Table 7: *Raw Experimental data on the drag force from the temperature range of 40°C to 60°C*

Temperature of Fluid (°C) ±0.2	Trials (x_i)	Drag Force (mN) ±0.0005
70	1	4.4196
	2	4.4226
	3	4.4246
	4	4.4266
	5	4.4296
80	1	4.3616
	2	4.3646
	3	4.3666
	4	4.3686
	5	4.3716
90	1	4.3116
	2	4.3146
	3	4.3166
	4	4.3186
	5	4.3216

Table 8: *Raw Experimental data on the drag force from the temperature range of 70°C to 90°C*